Title

CpG expedites regression of local and systemic tumors when combined with activatable nanodelivery.

Journal

Journal of controlled release : official journal of the Controlled Release Society, 220(Pt A)

ISSN

0168-3659

Authors

Kheirolomoom, Azadeh
Ingham, Elizabeth S
Mahakian, Lisa M
et al.

Publication Date

2015-12-01

DOI

10.1016/j.jconrel.2015.10.016

Peer reviewed

HHS Public Access

Author manuscript

J Control Release. Author manuscript; available in PMC 2016 December 28.

Published in final edited form as:

J Control Release. 2015 December 28; 220(0 0): 253–264. doi:10.1016/j.jconrel.2015.10.016.

CpG expedites regression of local and systemic tumors when combined with activatable nanodelivery

Azadeh Kheirolomoom[a,1], **Elizabeth S. Ingham**[a,1], **Lisa M. Mahakian**[a], **Sarah M. Tam**[a], **Matthew T. Silvestrini**[a], **Spencer K. Tumbale**[a], **Josquin Foiret**[a], **Neil E. Hubbard**[b], **Alexander D. Borowsky**[b], **William J. Murphy**[c], and **Katherine W. Ferrara**[a,*]

[a]University of California, Davis, Department of Biomedical Engineering, 451 East Health Sciences Drive, Davis, CA 95616, USA

[b]University of California, Davis, Center for Comparative Medicine, Davis, CA 95616, USA

[c]University of California, Davis, Department of Dermatology, 2921 Stockton Blvd., Institute for Regenerative Cures, Suite 1630, Sacramento, CA 95817, USA

Abstract

Ultrasonic activation of nanoparticles provides the opportunity to deliver a large fraction of the injected dose to insonified tumors and produce a complete local response. Here, we evaluate whether the local and systemic response to chemotherapy can be enhanced by combining such a therapy with locally-administered CpG as an immune adjuvant. In order to create stable, activatable particles, a complex between copper and doxorubicin (CuDox) was created within temperature-sensitive liposomes. Whereas insonation of the CuDox liposomes alone has been shown to produce a complete response in murine breast cancer after 8 treatments of 6 mg/kg delivered over 4 weeks, combining this treatment with CpG resolved local cancers within 3 treatments delivered over 7 days. Further, contralateral tumors regressed as a result of the combined treatment, and survival was extended in systemic disease. In both the treated and contralateral tumor site, the combined treatment increased leukocytes and CD4+ and CD8+ T-effector cells and reduced myeloid-derived suppressor cells (MDSCs). Taken together, the results suggest that this combinatorial treatment significantly enhances the systemic efficacy of locally-activated nanotherapy.

Graphical Abstract

*Corresponding author: Katherine W. Ferrara, PhD, Distinguished Professor, Department of Biomedical Engineering, One Shields Ave, University of California, Davis, Davis, CA 95616, USA, Phone: (530)754-9436, FAX: (530)754-5739, kwferrara@ucdavis.edu.
[1]These two authors contributed equally to this work.

Conflict of Interest: The authors declare no competing financial interest.

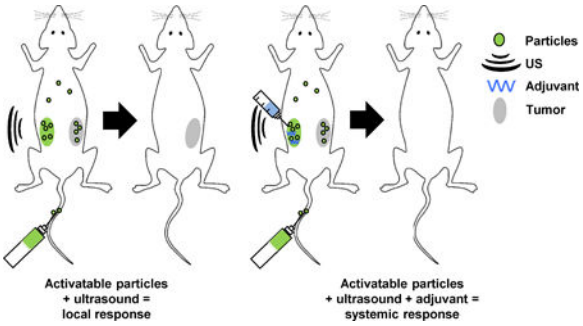

Keywords

CpG; Doxorubicin; Temperature-Sensitive Liposome; Ultrasound; Immunotherapy

1. Introduction

The use of ultrasound (US) and other local therapies has long been acknowledged to have the potential to cure local cancers; however, only a subset of lesions can be addressed by US, and treatment of inaccessible disease sites or large numbers of lesions is often required to increase life expectancy. The literature supports the use of US to reduce tumor tolerance or enhance immune response although these effects alone are not sufficient to generate a complete response [1–3]. The combination of US, immunomodulatory agents and chemotherapy has not been explored but is a rational choice because of the effect of US on the immune environment [4] and the augmented antitumor effects observed when chemotherapy is added to immunotherapy [5–7]. Recently, the addition of immune adjuvants to such local therapies has been shown to create an abscopal response and enhance survival [8, 9]. This represents a particularly significant opportunity for US methods as US can be applied repeatedly without a limit on the number of treatments and with a schedule that can be determined by biological need. With a protocol in which the accessible lesions are insonified and a systemic response is achieved, new treatment opportunities exist. Within this new paradigm, there are several potential directions: for example, US can be used to enhance local delivery via drug release or to ablate a lesion within a single treatment. Given the opportunity to repeatedly stimulate the immune system using a combination of US-mediated drug release and the application of immune adjuvants, we follow this approach here.

One strategy to achieve a minimally-toxic and highly-effective local treatment, which can be combined with immunotherapy, is to create an activatable particle that minimizes systemic toxicity and maximizes local tumor cell death. Previously, we formulated a highly-stable, pH-sensitive complex between doxorubicin (Dox) and copper (CuDox) in the core of lysolipid-containing temperature-sensitive liposomes (TSL) [10]. Local release of chemotherapy from temperature-sensitive particles has been shown to deliver a large fraction of the injected dose to the tumor [11]. When combined with US, a single administration of CuDox-TSL suppressed tumor growth, and further, with 8 repeated administrations, achieved a complete local tumor response with minimal systemic toxicity.

Repeated administration over a 4-week period was curative for local disease; however, this treatment did not extend survival in disseminated disease.

Chemotherapeutic drugs augment the antitumor effects of immunotherapies, where chemotherapy-induced apoptosis of tumor cells activates dendritic cells (DCs) and provides tumor-specific antigens for cross-presentation to T cells [12–17]. An advantage of therapy with temperature-sensitive particles is that the released drug is internalized or cleared quickly (thus recruited T cells/DCs survive). Further, this therapy is repeated several times in order to achieve a local cure. Such a protocol is ideal for the addition of immunotherapy [3, 18–22].

In our studies, we add the agonist CpG (single-stranded synthetic DNA molecules that contain cytosine “C” followed by a guanine “G” connected through a phosphodiester or phosphorothioate backbone) to enhance the response to systemic/metastatic cancers. Bacterial CpG DNA motifs that signal through Toll-like receptor 9 (TLR-9) have been used in combination with various vaccination strategies to treat cancer [23]. CpG signaling results in plasmacytoid DC activation, production of IFN-γ, DC maturation and T cell activation [23, 24]. Combining treatment with CpG agonists shows promise to extend local treatment to a systemic effect [25–28]. TLR agonists combined with local therapies have been the most successful such combination in creating a DC vaccine; alternatively cytotoxic T-lymphocyte-associated protein 4 (CTLA4) and programmed cell death (PD)-1 have not shown as potent of a synergistic effect with local therapies [25–28].

Therefore, in this study, we evaluated the use of CpG immunogenicity in combination with an US-releasable temperature-sensitive particle (CuDox-TSL) as a non-invasive local-cancer treatment with potential systemic antitumor effects in an aggressive murine breast cancer model. In order to evaluate both local and distant therapeutic effect, a bilaterally-transplanted NDL tumor model was employed in which one tumor per animal received direct US and CpG treatment. In this context, the power of immune adjuvants and activatable particles is combined for systemic therapy.

2. Material and methods

2.1. Materials

Doxorubicin hydrochloride (USP grade), copper (II) gluconate, ammonium sulfate, and triethanolamine (TEA) were purchased from Sigma (St. Louis, MO). 1,2-dipalmitoyl-sn-glycero-3-phosphocholine (DPPC), 1-palmitoyl-2-hydroxy-*sn*-glycero-3-phosphocholine (MPPC), and 1,2 distearoyl-sn-glycero-3-phosphoethanolamine-N-Methoxypolyethyleneglycol-2000 (DSPE-PEG2k) were obtained from Avanti Polar Lipids Inc. (Alabaster, AL). CpG-ODN 1826 (5′-tccatgacgttcctgacgtt-3′; total backbone phosphorothioated) was from InvivoGen (San Diego, CA). The *neu* deletion (NDL) metastatic mammary carcinoma cell line was obtained from the Alexander Borowsky Laboratory (UC Davis) [29, 30].

2.2. Preparation of liposomes and Dox loading

Lysolipid-containing temperature-sensitive liposomes (TSL) were made from DPPC:DSPE-PEG2k:MPPC (86:4:10, molar ratio). Liposomes were prepared by the hydration and extrusion method as described previously [10, 31]. Lipids, at the indicated ratios, were dissolved in chloroform. The chloroform was removed under a gentle stream of nitrogen gas and, subsequently, the residual solvent was removed under vacuum overnight. The dried lipid was hydrated in 0.3 mL of 100 mM copper (II) gluconate including triethanolamine at 540 mM (pH 8.4) to prepare copper-TSL (Cu-TSL). The multi-lamellar lipid solution at a final concentration of 50 mg/mL was extruded above the phase transition temperature of the lipid mixture through a polycarbonate membrane with a pore diameter of 100 nm. Cu-TSL were separated from non-encapsulated copper/TEA by passing the extruded liposomal suspension through a spin column of Sephadex G-75 (5 × 1 cm, GE Healthcare, Biosciences, Piscataway, NJ) equilibrated with saline (0.9% sodium chloride). The liposomal diameters were ~100 nm (115 nm ± 18 nm) as measured using a NICOMP™ 380 ZLS submicron particle analyzer (Particle Sizing System Inc., Santa Barbara, CA). Lipid concentration was measured using the Phospholipids C assay kit (Wako Chemicals USA, Richmond, VA) according to manufacturer's instructions. Dox was added to Cu-TSL at a drug-to-lipid ratio of 0.2:1 (wt:wt) and incubated at 37 °C for 1.5 h. The resulting CuDox-TSL were then separated from non-encapsulated Dox using Sephadex G-75 spin columns.

2.3. Animals and in vivo procedures

All animal experiments were conducted according to guidelines approved by the University of California, Davis, Animal Care and Use Committee (IACUC) and additional details of the study are provided in the supplementary information. FVB/n mice (Charles River, Wilmington, MA) were orthotopically transplanted with NDL tumor biopsies into the bilateral #4 inguinal mammary fat pads as previously described [32]. Mice were randomized among several groups including CuDox-TSL+US+CpG (CuDox+US+CpG), CuDox-TSL +US (CuDox+US), US+CpG (US+CpG), US only (US), drug treatment only (CuDox), CpG only (CpG) and no treatment (Control). A total of 101 bilateral NDL-tumor bearing mice were studied, among which the treatment groups for each study contained the following samples sizes: 1) 10-day tumor growth study: Control (n = 15), US (n = 3), CuDox (n = 8), CuDox+US (n = 9), CpG 30 μg (n = 3), CpG 50 μg (n = 3), CpG 60 μg (n = 3), CpG 100 μg (n = 3), US+CpG (n = 4), and CuDox+US+CpG (n = 9); 2) Immuno-profiling study: Control (n = 6), CpG (n = 4), US+CpG (n = 4), CuDox+US (n = 4), CuDox+US+CpG (n = 4); 3) Open-ended survival study: Control (n = 4), CpG (n = 7), US+CpG (n = 4), CuDox+US +CpG (n = 4). Drug-treated mice bearing bilateral NDL tumors of ~2 to 4 mm (~ 4 – 30 mm^3) in longitudinal diameter were injected via the tail vein with CuDox-TSL (~6 mg Dox/kg body weight and ~30 mg lipid/kg body weight) on days 0 and 3 (for the 7-day treatment period) and days 0, 3 and 7 (for the 10-day treatment period), with a total Dox injected dose of 100 mg/m^2. Non-drug treated control mice received a saline injection; 150 μL of 0.9% sodium chloride intravenously and/or 50 μL intratumorally were each evaluated and combined into the control group as no significant difference was observed. For treatments involving CpG, the dose of CpG was injected in 50 μL of endotoxin-free water intratumorally in a single injection (CpG only) or to the treated tumor immediately following US-hyperthermia (US+CpG and CuDox+US+CpG). For all insonified mice, one

tumor per animal was insonified for 5 min at 42 °C prior to intravenous administration of drug and saline in the drug treatment with US and US-only groups, respectively. Tumor insonation was continued for an additional 20 min at 42 °C after injection, and CpG was injected into the insonified tumor (Fig. 1A). The US protocol consisted of 100-cycle bursts at a 1.54 MHz center frequency and 1.1 MPa peak negative pressure, with the pulse-repetition frequency (PRF) ranging from 100 Hz to 5 kHz and maintained as controlled by a proportional integral derivative (PID) controller based on the constant temperature of 42 °C.

2.4. Antibodies

The following fluorochrome-conjugated monoclonal antibodies (mAbs) were purchased from BioLegend (San Diego, CA): Pacific blue (PB)-anti-CD45 (30-F11), fluorescein isothiocyanate (FITC)-anti-F4/80 (BM8), phycoerythrin (PE)-anti-NK1.1 (PK136), PE-Cy7-anti-CD3 (145-2C11), PE-Cy7-anti-CD11c (N418), allophycocyanin (APC)-CD206 (C068C2), APC-Cy7-anti-CD11b (M1/70), APC-Cy7-anti-CD25 (PC61), Alexa Fluor (AF)-700-anti-CD8 (53-6.7), AF-700-anti-Ly6G/Ly6C (Gr-1, RB6-8C5); from BD Biosciences (San Jose, CA): FITC-anti-CD4 (GK1.5), PE-anti-CD86 (GL1); and from eBioscience (San Diego, CA): PE-anti-Foxp3 (FJK-16s), PE-Cy5-anti-MHCII (M5/114.15.2). Isotype-matched mouse, rat and hamster IgG mAbs were used as negative staining controls. In order to block FcγIII/II receptor-mediated unspecific binding, the anti-CD16/CD32 antibody (2.4G2) from BD Biosciences was used.

2.5. Cell preparation and flow cytometry

Bilateral tumor-bearing mice were sacrificed after the 7-day treatment period for immune cell profiling via flow cytometry. In this syngeneic orthotopic model, a draining lymph node is located within the mammary inguinal fat pad containing the transplanted NDL tumor. Therefore, the entire fat pad containing the tumor and inguinal lymph node was collected and processed together for these analyses. Single-cell suspensions were obtained by mechanical disruption of the tissue followed by enzymatic digestion with 1mg/mL collagenase IV (Sigma Aldrich, St. Louis, MO) and filtration through a 70 μm cell strainer (BD Biosciences, San Jose, CA). Cell suspensions were stained using the LIVE/DEAD® Fixable Aqua Dead Cell Stain Kit (Invitrogen, Carlsbad, CA) according to the manufacturer's instructions in order to exclude dead cells from analysis. Cells were then incubated with 2.4G2 mAb for 10 min to block nonspecific antibody binding and finally stained with combinations of the indicated fluorochrome-conjugated anti-mouse antibodies for 25 min at 4 °C. Antibody combinations used to distinguish immune cell populations were $CD45^+$ (leukocytes) plus the following: $CD3^+$, $CD4^+$ (CD4+ T cells), $CD3^+$, $CD8^+$ (CD8+ T cells), $CD4^+$, $CD25^+$, $Foxp3^+$ (regulatory T cells), $CD11b^+$, $F4/80^+$, $Gr\text{-}1^-$ (macrophages), $CD11b^+$, $F4/80^+$, $Gr\text{-}1^-$, $CD86^+$, $MHCII^{hi}$ (M1 macrophages), $CD11b^+$, $F4/80^+$, $Gr\text{-}1^-$, $CD206^+$, $MHCII^{low}$ (M2 macrophages), $CD11c^+$, $MHCII^+$, $F4/80^-$ (dendritic cells), $CD3^-$, $NK1.1^+$ (natural killer cells) and $CD11b^+$, $Gr\text{-}1^+$ (myeloid derived suppressor cells). Intracellular mouse Foxp3 staining was carried out using the eBioscience Anti-Mouse/Rat Foxp3 Staining Set (72-5775) following manufacturer's instructions. All cell preparations were fixed in Cytofix buffer (BD Biosciences) diluted to 1% paraformaldehyde (PFA) in phosphate buffered saline (PBS). Stained cells were analyzed within 24 h on a

LSRII flow cytometer (BD, San Jose, CA) and all datasets were analyzed using FlowJo software vX (TreeStar).

IFN-γ secretion from CD4+ and CD8+ T cells was quantified using the Mouse IFN-γ Secretion Assay Cell Enrichment and Detection Kit (130-090-517, Miltenyi Biotec, San Diego, CA) according to the manufacturer's instructions, except cells were not magnetically labeled and enriched over a MACS column. Instead, after addition of the IFN-γ catch reagent to cells, followed by incubation in the recommended culture medium for 45 min at 37 °C, cells were washed and incubated with PE-anti-IFN-γ detection antibody in combination with the helper and cytotoxic T-cell fluorochrome-conjugated antibodies indicated above for 15 min at 4 °C. Finally, cells were washed, fixed in 1% PFA Cytofix buffer and run on a LSR II cytometer.

2.6. Statistical analyses

Statistical analyses were performed using Prism 6 software (GraphPad Software Inc.). Data are expressed as mean ± SEM, unless otherwise indicated. For analysis of three or more groups, a one-way ANOVA test was performed with either a Bonferroni or Tukey's post-hoc test as stated. Analysis of differences between two normally-distributed test groups was performed using an unpaired *t* test assuming unequal variance. For *t* tests comparing only two groups within a larger data set, the mean of each treatment group was compared only to the mean of the control group and a Sidak-Bonferroni correction for multiple comparisons was applied. Differences between groups in the Kaplan-Meier plot were determined using Log-rank statistics. P-values less than 0.05 were considered significant.

3. Results

3.1. In vivo efficacy achieved by combining CuDox-TSL, US and CpG

We augmented the CuDox+US treatment described previously [10, 31] by adding an intratumoral injection of CpG immediately following insonation (n=101) (Fig. 1A). Over the course of three treatments delivered on days 0, 3 and 7, treatment groups that included CuDox-TSL injection (CuDox, CuDox+US, CuDox+US+CpG) all suppressed tumor growth compared to control animals (Fig. 1B). CuDox+US+CpG treatment resulted in tumor regression after the first treatment and tumor growth was reduced to the greatest extent with CuDox+US+CpG as compared with CuDox+US or CuDox alone (each $p < 0.001$ compared to control, Fig. 1B, D and SI Fig. S1). The reduction in tumor growth achieved by CuDox +US+CpG was also observed in the contralateral tumors (Fig. 1B, D, $p < 0.001$). While treatment with US-hyperthermia only did not affect tumor growth, intratumoral administration of CpG alone or CpG in combination with US-hyperthermia did reduce growth in directly-injected tumors and to a lesser extent in contralateral tumors (Fig. 1C, $p < 0.01$ for CpG-treated tumors compared to control and $p < 0.001$ for US+CpG treated tumors compared to control). The antitumor effect of CpG did not significantly increase with increasing injected dose (Fig. 1C).

In order to assess the variability of response, we also present the individual tumor growth curves from all mice evaluated with the CuDox+US+CpG, CpG and control protocols (Fig. 1E–I). For the directly treated CuDox+US+CpG treatment group, tumor regression was

observed immediately in 9 of 12 mice (Fig. 1E), whereas the remaining 3 of 12 did not grow or grew slowly initially and decreased in volume after the third treatment. For the CuDox +US+CpG contralateral group, 10 of 11 tumors grew initially; however, tumor volume was decreasing in 11 of the 12 after three treatments (Fig. 1F). This consistency in treatment response was not observed with administration of CpG alone (Fig. 1G, H); and tumor growth continued in 3 of 9 directly treated tumors and 4 of 10 contralateral tumors after three treatments. Control animals did not receive any treatment and therefore both bilateral tumors were considered untreated control tumors (*i.e.* there is no “primary” and “contralateral” tumor in these animals).

H&E-stained tumor sections obtained on day 10 confirmed a dramatic reduction in viable tumor cells remaining after the combinatorial treatment with CuDox+US+CpG compared to control tumors (Fig. 2). This reduced cell viability was also apparent in the contralateral tumors of mice receiving the CuDox+US+CpG treatment, with infiltrating leukocytes elevated and extensive necrosis observed. Similarly, histological sections obtained from tumors treated with CpG alone also displayed an increase in leukocytes and tumor cell apoptosis, but with a lesser overall effect in the contralateral tumors of this group of mice. Mice receiving CuDox only or CuDox+US treatment displayed the greatest tumor viability in both the treated and contralateral tumors.

3.2. Immune cell profiles in the tumor-containing inguinal fat pad after CuDox+US+CpG treatment

Immune cells were quantified by flow cytometry after two treatments delivered on days 0 and 3. The percentage of total cells expressing CD45 (general leukocytes) at the site of the inguinal fat pad containing tumor and lymph node was significantly increased in the US +CpG-, CuDox+US- and CuDox+US+CpG-treated tumor site and in the contralateral tumor site of CuDox+US+CpG-treated mice (Fig. 3A, left column, $p < 0.05$). Because these treatments dramatically reduced tumor growth and therefore total cell number, the total leukocyte number in the directly-treated and contralateral tumor sites of these animals was not significantly different compared to controls (Fig. 3A, right column). The fraction of CD4+ and CD8+ T cells in both the treated and contralateral tumor sites of CuDox+US +CpG-treated mice was increased compared to control mice (Fig. 3B, C, $p < 0.001$ for CD4+ T cells in the treated and contralateral site and CD8+ T cells in the treated site; $p < 0.05$ for CD8+ T cells in the contralateral site). CuDox+US treatment on its own also significantly increased the fraction of CD4+ T cells, but only in the treated-tumor site (Fig. 3B). Further, the fraction of macrophages within the treated site was significantly increased with local CuDox+US+CpG treatment, but not with other treatments (Fig. 3B, $p < 0.05$). For all treatments, the M1 macrophage phenotype was more common than the M2 phenotype (M1 macrophage frequency was 19.4 ± 11.1% of total macrophages versus 3.5 ± 3.0% for M2 macrophages, mean ± SD); however, most of the fat pad and tumor macrophages did not demonstrate either the M1 or M2 markers. No significant difference in the frequencies of M2 macrophages, dendritic cells or natural killer cells was noted with any treatment compared to controls (data not shown).

3.3. Reduced immunosuppression and enhanced T cell activation after CuDox+US+CpG treatment

A significant reduction in the frequency and absolute number of myeloid-derived suppressor cells (MDSCs) within CuDox+US+CpG-treated and contralateral tumor sites was observed at the termination of the 7-day treatment period (Fig. 4A through C, $p < 0.05$). In control tumors, Foxp3-staining regulatory T cells (Tregs) were found to be strongly associated with the tumor periphery (Fig. 4D). In contrast, for mice treated with CuDox+US+CpG, Tregs were significantly reduced in the treated tumors but remained in the contralateral tumor periphery in mice with remaining viable tumor (Fig. 4D, E, $p = 0.034$). Tregs were also quantified in the tumor periphery of CpG-only treated and contralateral tumors. However, we did not observe a significant difference in the Treg populations within the tumor periphery of these treated and contralateral tumors compared to that of the control (data not shown).

CuDox+US+CpG treatment also increased CD4+ T cell and CD8+ T cell activation, as indicated by significantly higher percentages of IFN-γ secreting CD4+ T cells in the locally-treated tumor site and significantly higher percentages of IFN-γ secreting CD8+ T cells within both the locally-treated and contralateral tumor sites compared to those of control mice (Fig. 5A, B, ** $p < 0.01$, *** $p < 0.001$).

3.4. Treatment with CuDox+US+CpG elicits tumor remission and extends survival

In mice receiving CuDox+US+CpG, complete tumor regression was observed 20 days after treatment termination. Further, only the directly-treated CuDox+US+CpG tumors maintained complete remission over the entire 48 days of monitoring (Fig. 6A). Survival was significantly extended only with the combinatorial CuDox+US+CpG treatment ($p < 0.05$, compared to control, Fig. 6B). Growth of the contralateral tumors limited survival in the CuDox+US+CpG treatment group, but we reiterate that long-term survival has previously been achieved when all tumors are directly treated with repeated CuDox+US [10]. Survival percentages were similar for US+CpG and CpG-only treated mice (data not shown). With CpG administration following CuDox+US, all locally-treated tumors showed consistent and sustainable tumor-regression over the 48-day study and reduced growth of the contralateral tumors (SI, Fig. S2A, S2B). This consistency in treatment response was not observed with administration of CpG alone or with the US+CpG treatment (SI, Fig. S2C–F). Histology of the tumor and surrounding fat pad obtained upon sacrifice after up to 48 days post treatment confirmed complete tumor regression in CuDox+US+CpG-treated mice (Fig. 6C, i–iv), where viable tumor cells were not detected in the directly-treated fat pads of these animals; however, inflammation is apparent in the form of reaction within the lymph node (yellow arrow) and surrounding parenchyma. Control tumors (Fig. 6C, viii), CuDox+US +CpG contralateral tumors and CpG-only treated and contralateral tumors contained regions with viable tumor (Fig. 6C, v, vi, and vii, respectively).

3.5. Systemic toxicity with repeated CuDox+US+CpG treatment

We monitored animal body weight, organ hypertrophy, and blood hematology and circulating proteins as indicators of kidney and liver function. As shown in Supplementary Fig. S3A, body weight was reduced by 5% in the CuDox+US+CpG group over the initial 10

days of treatment; however, normal weight gain returned upon treatment termination. Although mice receiving CuDox+US+CpG treatment exhibited hepatomegaly immediately following the 10-day treatment period, upon termination of the 48-day study period, liver hypertrophy was not detected and spleen and heart weights were similar to no-treatment control animals (data not shown). Leukopenia was also observed in CuDox+US+CpG treated mice over the 10-day treatment period (SI, Fig. S3B, $p < 0.01$). However, once treatment was terminated, white blood cell levels recovered by the end of the 48-day study (SI, Fig. S3B).

4. Discussion

US was applied to locally release a drug from temperature-sensitive particles and provided a real-time and image-guided means of delivering a precise and focused thermal dose. Historically, a major concern for such activatable therapies has been the inability to impact systemic cancers. Here, we demonstrate that the impact of such therapies can be extended to treat systemic disease. The low systemic toxicity and highly localized delivery demonstrated here represents a new approach to trigger an *in situ* tumor vaccine. While we have not yet optimized the timing and protocol for this combined treatment, we found that a systemic effect was observed after three treatments and survival was extended.

With addition of the Toll-like receptor agonist, CpG, to the CuDox+US combinatorial treatment, complete regression of the local tumor was achieved with fewer treatments than with the CuDox+US treatment alone (3 treatments over 10 days vs 8 treatments over 4 weeks). Viable tumor was not detected by histology within the directly-treated tumors; viability of the contralateral tumors was confirmed to be reduced on histological examination after 10 days of treatment and therefore survival was extended. The rapid and complete destruction of the primary tumor raises interesting questions for an immunotherapy protocol as the contralateral tumor was responding but had not been eliminated. Since CpG is typically locally administered within viable tumor and the three CuDox+US+CpG treatments eliminated all local viable tumor, extending treatment of the initial primary lesion beyond the first three treatments is expected to be suboptimal for inducing a systemic response. A more effective systemic therapy (and enhanced survival) may require the direct treatment of multiple tumors or metastases.

Release of Dox from CuDox-TSL was previously shown to produce a complete local response in syngeneic breast tumors [10]. Full release of the Dox requires release of the complex from the particle and a reduction in pH in order to disassociate the copper and Dox. With the ability to selectively release chemotherapy in tumors and eliminate local disease, we sought to extend the therapeutic effect to systemic cancer by adding an immune adjuvant to the treatment. The advantage of this approach, as compared with traditional chemotherapy or radiation treatment, is the highly-localized delivery and resultant low-systemic toxicity. Thus, a tailored protocol could be applied to multiple sites and repeated as needed to enhance systemic efficacy.

The combined treatment was well tolerated. We observed significant leukopenia in all CpG-treated animals, reduced body weight and increased hepatomegaly immediately after the

treatment protocol. However, these changes disappeared within several weeks of treatment termination.

Changes in immune cell numbers and phenotype

CpG is known to be an effective stimulator of Toll-like receptor 9 (TLR-9), which can trigger proliferation and activation of T lymphocyte inflammatory antitumor responses in murine models both directly [33] and indirectly through antigen-presenting cells (APCs) [34]. Here, we found that macrophage frequencies were significantly increased in the directly-treated tumor site of CuDox+US+CpG-treated animals, suggesting triggering of an innate immune response by combinatorial drug-CpG administration. It is important to note that the CuDox+US+CpG treatment did not enhance the frequency of M2-polarized macrophages, which are thought to be involved in promoting tumor protection and immune evasion [35–37]. We also observed a significant increase in the frequencies of leukocytes in CuDox+US+CpG-treated and contralateral tumors, of which, CD4+ and CD8+ T cells were significantly amplified.

These data suggest that the heightened efficacy of the CpG-augmented therapy may be mediated, at least in part, via enriched activation of the innate immune system, in terms of APCs such as macrophages, and possibly even the adaptive-immune system through T lymphocyte activity. Data have suggested that a rapid infiltration of T cells in primary tumor lesions is a positive prognostic factor in melanoma [38], ovarian cancer [39], renal cell carcinoma [40], bladder cancer [41], and several other solid cancers [42]. CD4+ T cells are known to orchestrate a broad range of immune responses and are equipped to differentiate into multiple sub-lineages that can induce and maintain destructive immune responses to self-antigens, including tumor antigens. Working in conjunction with CD4+ T cells, CD8+ T cells can directly target and exert potent tumor-killing activity [40, 41].

The response to CpG-only and US+CpG treatments was not consistent within the treatment groups. However, when CpG is administered following CuDox+US, all locally-treated tumors displayed highly effective tumor suppression within a much shorter time period than expected or observed for treatment with doxorubicin alone or with CuDox+US. The consistent, sustained responses achieved with the CuDox+US+CpG treatment may indicate that there is an antigen-specific response occurring, as opposed to what might be a more non-specific inflammatory immune response generated by CpG with and without US in the absence of drug. This will require additional studies to tease apart these issues.

Reduction in the immunosuppressive environment

A major obstacle to successful cancer immunotherapy is the suppression of effector cells that is induced by the tumor microenvironment. The accumulation of myeloid-derived suppressor cells (MDSCs) has been recognized as a major mechanism in the promotion of tumor-induced immune suppression [43–45]. In mice, these cells are broadly defined by their unique coexpression of macrophage (CD11b) and granulocyte (Gr-1) markers [43], and they possess the ability to suppress T cell antitumor responses in antigen-specific or nonspecific manners depending on the condition of T cell activation [46, 47]. Here we found that the CuDox+US+CpG combinatorial therapy significantly reduced the percentage and

absolute number of MDSCs in both the locally-treated tumor site and the contralateral tumor site. Further, significant increases in the frequencies of T lymphocytes actively secreting IFN-γ were observed in the CuDox+US+CpG-treated (IFN-γ producing CD4+ and CD8+ T cells) and contralateral tumor sites (IFN-γ producing CD8+ T cells), but not in the tumor sites of any other treatments tested, compared to controls. IFN-γ is produced by certain CD4+ T cell subsets and CD8+ T cells once antigen-specific immunity has developed and is associated with prominent antitumor activity [48, 49]. IFN-γ secretion promotes the priming and expansion of cytotoxic CD8+ T and natural killer (NK) cells and enhances the immunogenicity of tumor cells themselves. These results therefore suggest that the CpG-augmented treatment may enhance activation of T lymphocyte effectors, possibly through a reduction in inhibitory MDSCs.

Regulatory T cells (Tregs) are also vital down-regulators of inflammatory immune responses, and studies with tumor mouse models have indicated a central negative role for Tregs in hindering efficient tumor eradication [50]. In this study, Tregs were distributed at the tumor periphery in untreated control tumors but were effectively eliminated in CuDox +US+CpG directly-treated tumors. The presence of Treg cells surrounding the contralateral tumor in animals treated with CuDox+US+CpG was correlated with the presence of viable tumor cells. Therefore, future work will incorporate strategies to further reduce the systemic Treg population.

5. Conclusion

In conclusion, we find that the combination of an activatable nanotherapy protocol with an immune adjuvant enhanced local nanotherapy efficacy while reducing systemic tumor growth and enhancing the anti-tumor immune response. Optimization of such treatments is complex but shows the potential to provide new treatment options for systemic cancers.

Supplementary Material

Refer to Web version on PubMed Central for supplementary material.

Acknowledgments

Funding was provided by NIHR01CA134659, NIHR01CA103828 and NIHR01CA199658.

References

1. Hu Z, Yang XY, Liu Y, Sankin GN, Pua EC, Morse MA, Lyerly HK, Clay TM, Zhong P. Investigation of HIFU-induced anti-tumor immunity in a murine tumor model. Journal of Translational Medicine. 2007; 5
2. Liu F, Hu Z, Qiu L, Hui C, Li C, Zhong P, Zhang J. Boosting high-intensity focused ultrasound-induced anti-tumor immunity using a sparse-scan strategy that can more effectively promote dendritic cell maturation. Journal of Translational Medicine. 2010; 8
3. Xu ZL, Zhu XQ, Lu P, Zhou Q, Zhang J, Wu F. Activation of tumor-infiltating antigen presenting cells by high intensity focused ultrasound ablation of human breast cancer. Ultrasound in Medicine and Biology. 2009; 35:50–57. [PubMed: 18950932]
4. Unga J, Hashida M. Ultrasound induced cancer immunotherapy. Advanced drug delivery reviews. 2014; 72:144–153. [PubMed: 24680708]

5. Weigel BJ, Rodeberg DA, Krieg AM, Blazar BR. CpG oligodeoxynucleotides potentiate the antitumor effects of chemotherapy or tumor resection in an orthotopic murine model of rhabdomyosarcoma. Clinical cancer research : an official journal of the American Association for Cancer Research. 2003; 9:3105–3114. [PubMed: 12912962]
6. Pratesi G, Petrangolini G, Tortoreto M, Addis A, Belluco S, Rossini A, Selleri S, Rumio C, Menard S, Balsari A. Therapeutic synergism of gemcitabine and CpG-oligodeoxynucleotides in an orthotopic human pancreatic carcinoma xenograft. Cancer Res. 2005; 65:6388–6393. [PubMed: 16024642]
7. Zhu J, He S, Du J, Wang Z, Li W, Chen X, Jiang W, Zheng D, Jin G. Local administration of a novel Toll-like receptor 7 agonist in combination with doxorubicin induces durable tumouricidal effects in a murine model of T cell lymphoma. Journal of hematology & oncology. 2015; 8:21. [PubMed: 25887995]
8. den Brok MH, Sutmuller RP, Nierkens S, Bennink EJ, Toonen LW, Figdor CG, Ruers TJ, Adema GJ. Synergy between in situ cryoablation and TLR9 stimulation results in a highly effective in vivo dendritic cell vaccine. Cancer Res. 2006; 66:7285–7292. [PubMed: 16849578]
9. Gameiro SR, Higgins JP, Dreher MR, Woods DL, Reddy G, Wood BJ, Guha C, Hodge JW. Combination therapy with local radiofrequency ablation and systemic vaccine enhances antitumor immunity and mediates local and distal tumor regression. PloS one. 2013; 8:e70417. [PubMed: 23894654]
10. Kheirolomoom A, Lai CY, Tam SM, Mahakian LM, Ingham ES, Watson KD, Ferrara KW. Complete regression of local cancer using temperature-sensitive liposomes combined with ultrasound-mediated hyperthermia. J Control Release. 2013; 172:266–273. [PubMed: 23994755]
11. Manzoor AA, Lindner LH, Landon CD, Park JY, Simnick AJ, Dreher MR, Das S, Hanna G, Park W, Chilkoti A, Koning GA, ten Hagen TLM, Needham D, Dewhirst MW. Overcoming Limitations in Nanoparticle Drug Delivery: Triggered, Intravascular Release to Improve Drug Penetration into Tumors. Cancer research. 2012; 72:5566–5575. [PubMed: 22952218]
12. Baxevanis C, Perez S, Papamichail M. Combinatorial treatments including vaccines, chemotherapy and monoclonal antibodies for cancer therapy, Cancer Immunology. Immunotherapy. 2009; 58:317–324.
13. Nowak AK, Lake RA, Marzo AL, Scott B, Heath WR, Collins EJ, Frelinger JA, Robinson BWS. Induction of Tumor Cell Apoptosis In Vivo Increases Tumor Antigen Cross-Presentation, Cross-Priming Rather than Cross-Tolerizing Host Tumor-Specific CD8 T Cells. The Journal of Immunology. 2003; 170:4905–4913. [PubMed: 12734333]
14. Steer HJ, Lake RA, Nowak AK, Robinson BWS. Harnessing the immune response to treat cancer. Oncogene. 2010; 29:6301–6313. [PubMed: 20856204]
15. Nowak AK, Robinson BWS, Lake RA. Synergy between Chemotherapy and Immunotherapy in the Treatment of Established Murine Solid Tumors. Cancer research. 2003; 63:4490–4496. [PubMed: 12907622]
16. Apetoh L, Ghiringhelli F, Tesniere A, Obeid M, Ortiz C, Criollo A, Mignot G, Maiuri MC, Ullrich E, Saulnier P, Yang H, Amigorena S, Ryffel B, Barrat FJ, Saftig P, Levi F, Lidereau R, Nogues C, Mira JP, Chompret A, Joulin V, Clavel-Chapelon F, Bourhis J, Andre F, Delaloge S, Tursz T, Kroemer G, Zitvogel L. Toll-like receptor 4-dependent contribution of the immune system to anticancer chemotherapy and radiotherapy. Nature medicine. 2007; 13:1050–1059.
17. Casares N, Pequignot MO, Tesniere A, Ghiringhelli F, Roux S, Chaput N, Schmitt E, Hamai A, Hervas-Stubbs S, Obeid M, Coutant F, Metivier D, Pichard E, Aucouturier P, Pierron G, Garrido C, Zitvogel L, Kroemer G. Caspase-dependent immunogenicity of doxorubicin-induced tumor cell death. The Journal of experimental medicine. 2005; 202:1691–1701. [PubMed: 16365148]
18. Wu F, Wang ZB, Cao YD, Zhou Q, Zhang Y, Xu ZL, Zhu XQ. Expression of tumor antigens and heat-shock protein 70 in breast cancer cells after high-intensity focused ultrasound ablation. Annals of Surgical Oncology. 2007; 14:1237–1242. [PubMed: 17187168]
19. Wu F, Zhou L, Chen WR. Host antitumour immune responses to HIFU ablation. International Journal of Hyperthermia. 2007; 23:165–171. [PubMed: 17578340]
20. Zhou Q, Zhu XQ, Zhang J, Xu ZL, Lu P, Wu F. Changes in circulating immunosuppressive cytokine levels of cancer patients after high intensity focused ultrasound treatment. Ultrasound in Medicine and Biology. 2008; 34:81–87. [PubMed: 17854983]

21. Zhong-Lin X, Xue-Qiang Z, Pei L, Qiang Z, Jun Z, Feng W. Activation of tumor-infiltrating antigen presenting cells by high intensity focused ultrasound ablation of human breast cancer. Ultrasound in Medicine and Biology. 2009; 35
22. Deng J, Zhang Y, Feng J, Wu F. Dendritic cells loaded with ultrasound-ablated tumor induce in vivo specific antitumor responses. Ultrasound in Medicine and Biology. 2010; 36:441–448. [PubMed: 20172447]
23. Jurk M, Vollmer J. Therapeutic Applications of Synthetic CpG Oligodeoxynucleotides as TLR9 Agonists for Immune Modulation. BioDrugs. 2007; 21:387–401. [PubMed: 18020622]
24. Higgins JP, Bernstein MB, Hodge JW. Enhancing immune responses to tumor-associated antigens. Cancer Biology & Therapy. 2009; 8:1440–1449. [PubMed: 19556848]
25. den Brok MH, Nierkens S, Wagenaars JA, Ruers TJ, Schrier CC, Rijke EO, Adema GJ. Saponin-based adjuvants create a highly effective anti-tumor vaccine when combined with in situ tumor destruction. Vaccine. 2012; 30:737–744. [PubMed: 22138178]
26. den Brok MHMGM, Sutmuller RPM, Nierkens S, Bennink EJ, Frielink C, Toonen LWJ, Boerman OC, Figdor CG, Ruers TJM, Adema GJ. Efficient loading of dendritic cells following cryo and radiofrequency ablation in combination with immune modulation induces anti-tumour immunity. Br J Cancer. 2006; 95:896–905. [PubMed: 16953240]
27. den Brok MHMGM, Sutmuller RPM, van der Voort R, Bennink EJ, Figdor CG, Ruers TJM, Adema GJ. In Situ Tumor Ablation Creates an Antigen Source for the Generation of Antitumor Immunity. Cancer research. 2004; 64:4024–4029. [PubMed: 15173017]
28. Nierkens S, den Brok MH, Garcia Z, Togher S, Wagenaars J, Wassink M, Boon L, Ruers TJ, Figdor CG, Schoenberger SP, Adema GJ, Janssen EM. Immune Adjuvant Efficacy of CpG Oligonucleotide in Cancer Treatment Is Founded Specifically upon TLR9 Function in Plasmacytoid Dendritic Cells. Cancer research. 2011; 71:6428–6437. [PubMed: 21788345]
29. Miller JK, Shattuck DL, Ingalla EQ, Yen LL, Borowsky AD, Young LJT, Cardiff RD, Carraway KL, Sweeney C. Suppression of the Negative Regulator LRIG1 Contributes to ErbB2 Overexpression in Breast Cancer. Cancer research. 2008; 68:8286–8294. [PubMed: 18922900]
30. Siegel PM, Ryan ED, Cardiff RD, Muller WJ. Elevated expression of activated forms of Neu/ErbB-2 and ErbB-3 are involved in the induction of mammary tumors in transgenic mice: implications for human breast cancer. Embo J. 1999; 18:2149–2164. [PubMed: 10205169]
31. Kheirolomoom A, Mahakian LM, Lai CY, Lindfors HA, Seo JW, Paoli EE, Watson KD, Haynam EM, Ingham ES, Xing L, Cheng RH, Borowsky AD, Cardiff RD, Ferrara KW. Copper-Doxorubicin as a Nanoparticle Cargo Retains Efficacy with Minimal Toxicity. Mol Pharm. 2010; 7:1948–1958. [PubMed: 20925429]
32. Borowsky AD, Namba R, Young LJ, Hunter KW, Hodgson JG, Tepper CG, McGoldrick ET, Muller WJ, Cardiff RD, Gregg JP. Syngeneic mouse mammary carcinoma cell lines: two closely related cell lines with divergent metastatic behavior. Clinical & experimental metastasis. 2005; 22:47–59. [PubMed: 16132578]
33. Bendigs S, Salzer U, Lipford GB, Wagner H, Heeg K. CpG-oligodeoxynucleotides co-stimulate primary T cells in the absence of antigen-presenting cells. European journal of immunology. 1999; 29:1209–1218. [PubMed: 10229088]
34. Sun S, Zhang X, Tough DF, Sprent J. Type I interferon-mediated stimulation of T cells by CpG DNA. The Journal of experimental medicine. 1998; 188:2335–2342. [PubMed: 9858519]
35. Kawamura K, Komohara Y, Takaishi K, Katabuchi H, Takeya M. Detection of M2 macrophages and colony-stimulating factor 1 expression in serous and mucinous ovarian epithelial tumors. Pathol Int. 2009; 59:300–305. [PubMed: 19432671]
36. Kurahara H, Shinchi H, Mataki Y, Maemura K, Noma H, Kubo F, Sakoda M, Ueno S, Natsugoe S, Takao S. Significance of M2-Polarized Tumor-Associated Macrophage in Pancreatic Cancer. J Surg Res. 2011; 167:E211–E219. [PubMed: 19765725]
37. Niino D, Komohara Y, Kimura Y, Takeuchi M, Miyoshi H, Yoshida M, Ichikawa A, Sugita Y, Takeya M, Kikuchi M, Nakamura S, Ohshima K. M2 Macrophage Infiltration Is Closely Associated with Poor Prognosis for Adult T-Cell Leukemia/Lymphoma (ATLL). Blood. 2011; 118:1569–1570.

38. Clark WH. Tumour progression and the nature of cancer. British journal of cancer. 1991; 64:631–644. [PubMed: 1911211]
39. Sato E, Olson SH, Ahn J, Bundy B, Nishikawa H, Qian F, Jungbluth AA, Frosina D, Gnjatic S, Ambrosone C, Kepner J, Odunsi T, Ritter G, Lele S, Chen YT, Ohtani H, Old LJ, Odunsi K. Intraepithelial CD8+ tumor-infiltrating lymphocytes and a high CD8+/regulatory T cell ratio are associated with favorable prognosis in ovarian cancer. Proceedings of the National Academy of Sciences of the United States of America. 2005; 102:18538–18543. [PubMed: 16344461]
40. Nakano O, Sato M, Naito Y, Suzuki K, Orikasa S, Aizawa M, Suzuki Y, Shintaku I, Nagura H, Ohtani H. Proliferative activity of intratumoral CD8(+) T-lymphocytes as a prognostic factor in human renal cell carcinoma: clinicopathologic demonstration of antitumor immunity. Cancer Res. 2001; 61:5132–5136. [PubMed: 11431351]
41. Sharma P, Shen Y, Wen S, Yamada S, Jungbluth AA, Gnjatic S, Bajorin DF, Reuter VE, Herr H, Old LJ, Sato E. CD8 tumor-infiltrating lymphocytes are predictive of survival in muscle-invasive urothelial carcinoma. Proceedings of the National Academy of Sciences of the United States of America. 2007; 104:3967–3972. [PubMed: 17360461]
42. Gooden MJ, de Bock GH, Leffers N, Daemen T, Nijman HW. The prognostic influence of tumour-infiltrating lymphocytes in cancer: a systematic review with meta-analysis. British journal of cancer. 2011; 105:93–103. [PubMed: 21629244]
43. Gabrilovich DI, Ostrand-Rosenberg S, Bronte V. Coordinated regulation of myeloid cells by tumours. Nature reviews Immunology. 2012; 12:253–268.
44. Ostrand-Rosenberg S, Sinha P, Beury DW, Clements VK. Cross-talk between myeloid-derived suppressor cells (MDSC), macrophages, and dendritic cells enhances tumor-induced immune suppression. Seminars in cancer biology. 2012; 22:275–281. [PubMed: 22313874]
45. Diaz-Montero CM, Salem ML, Nishimura MI, Garrett-Mayer E, Cole DJ, Montero AJ. Increased circulating myeloid-derived suppressor cells correlate with clinical cancer stage, metastatic tumor burden, and doxorubicin-cyclophosphamide chemotherapy, Cancer immunology. immunotherapy : CII. 2009; 58:49–59.
46. Kusmartsev S, Gabrilovich DI. Role of immature myeloid cells in mechanisms of immune evasion in cancer, Cancer immunology. immunotherapy : CII. 2006; 55:237–245.
47. Talmadge JE. Pathways mediating the expansion and immunosuppressive activity of myeloid-derived suppressor cells and their relevance to cancer therapy. Clinical cancer research : an official journal of the American Association for Cancer Research. 2007; 13:5243–5248. [PubMed: 17875751]
48. Kim HJ, Cantor H. CD4 T-cell subsets and tumor immunity: the helpful and the not-so-helpful. Cancer immunology research. 2014; 2:91–98. [PubMed: 24778273]
49. Ikeda H, Old LJ, Schreiber RD. The roles of IFN gamma in protection against tumor development and cancer immunoediting. Cytokine & growth factor reviews. 2002; 13:95–109. [PubMed: 11900986]
50. Sakaguchi S, Yamaguchi T, Nomura T, Ono M. Regulatory T cells and immune tolerance. Cell. 2008; 133:775–787. [PubMed: 18510923]

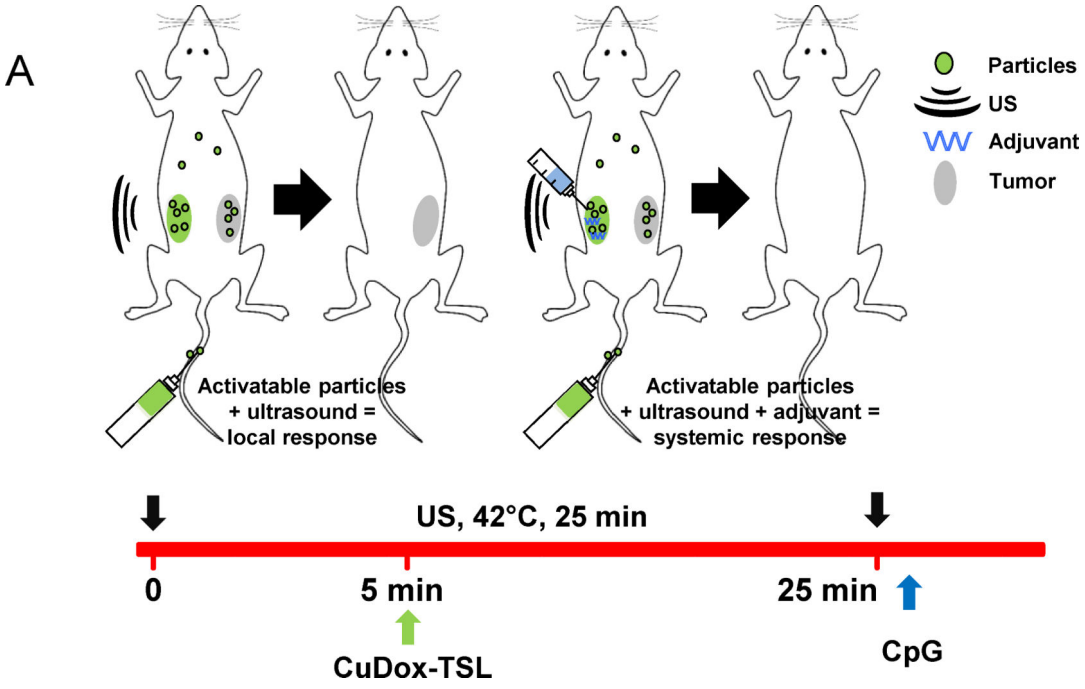

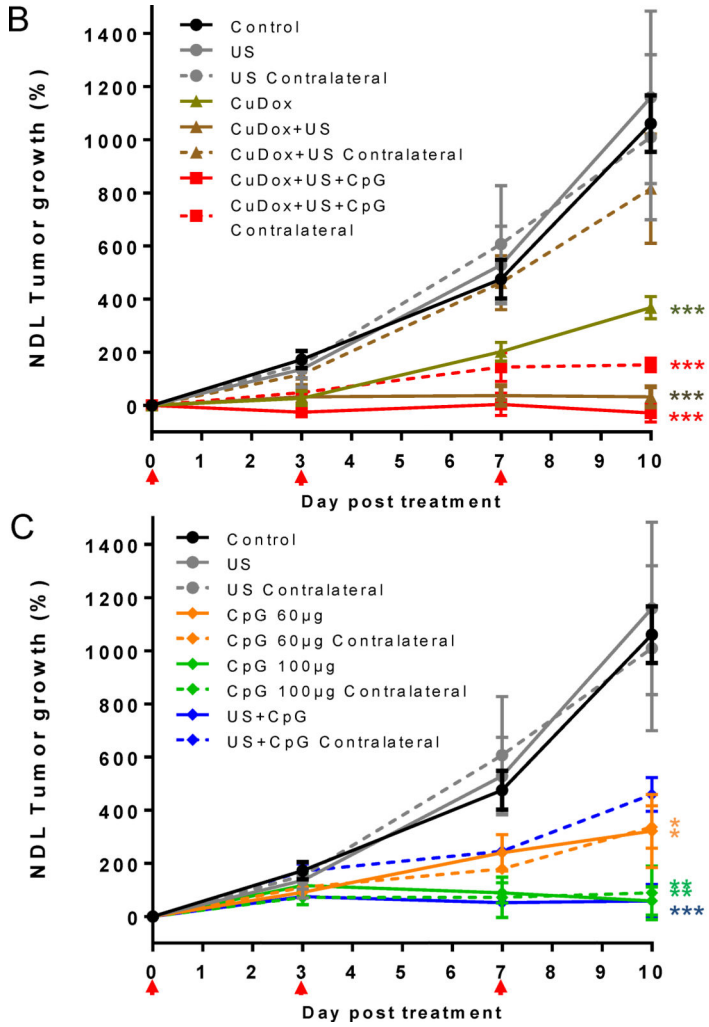

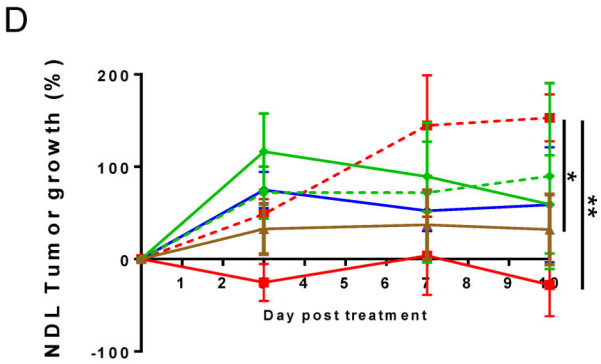

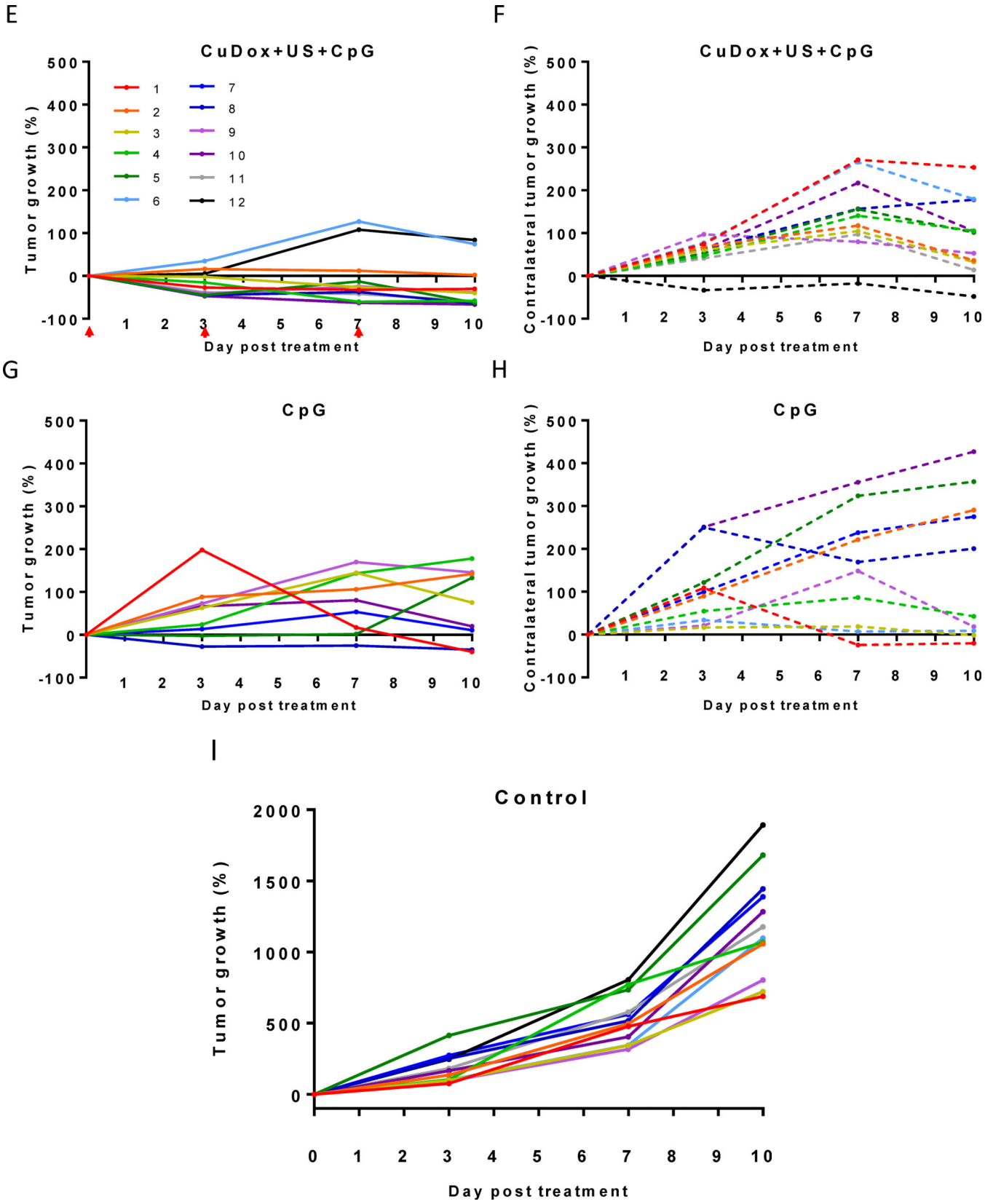

Fig. 1.

CpG reduces tumor growth in directly-treated and contralateral tumors. A: schematic of the treatment protocol. B–D: tumor growth shown as a function of days over the 10-day, 3-dose treatment cycle and presented as percent tumor growth. Initial tumor diameter was 2–4 mm. The sample size for each group was: Control (n = 15), US (n = 3), CuDox (n = 8), CuDox +US (n = 9), CpG 60ug (n = 3), CpG 100ug (n = 3), US+CpG (n = 4), and CuDox+US+CpG (n = 9). E–I: Plots of individual tumor growth rates in response to each treatment over the 10-day, 3-dose treatment period. These data combine those tumors obtained from both the 10-day tumor growth study and the open-ended survival study. Each mouse was injected intravenously with either saline or CuDox-TSL (~6 mg Dox/kg body weight) and, for animals receiving US, one tumor per animal was insonified to release the drug. Animals receiving CuDox+US+CpG or US+CpG treatment received an intratumoral injection of 100 μg of CpG immediately after tumor insonation. Animals receiving CpG-only received an intratumoral injection of either 60 or 100 μg CpG. Red arrows indicate treatment days. Data are shown as mean ± SEM, * $p < 0.05$, ** $p < 0.01$, *** $p < 0.001$, One-way ANOVA with Tukey's post-hoc correction (B and C, indicated significance is compared to control) or unpaired *t* test assuming unequal variance (D).

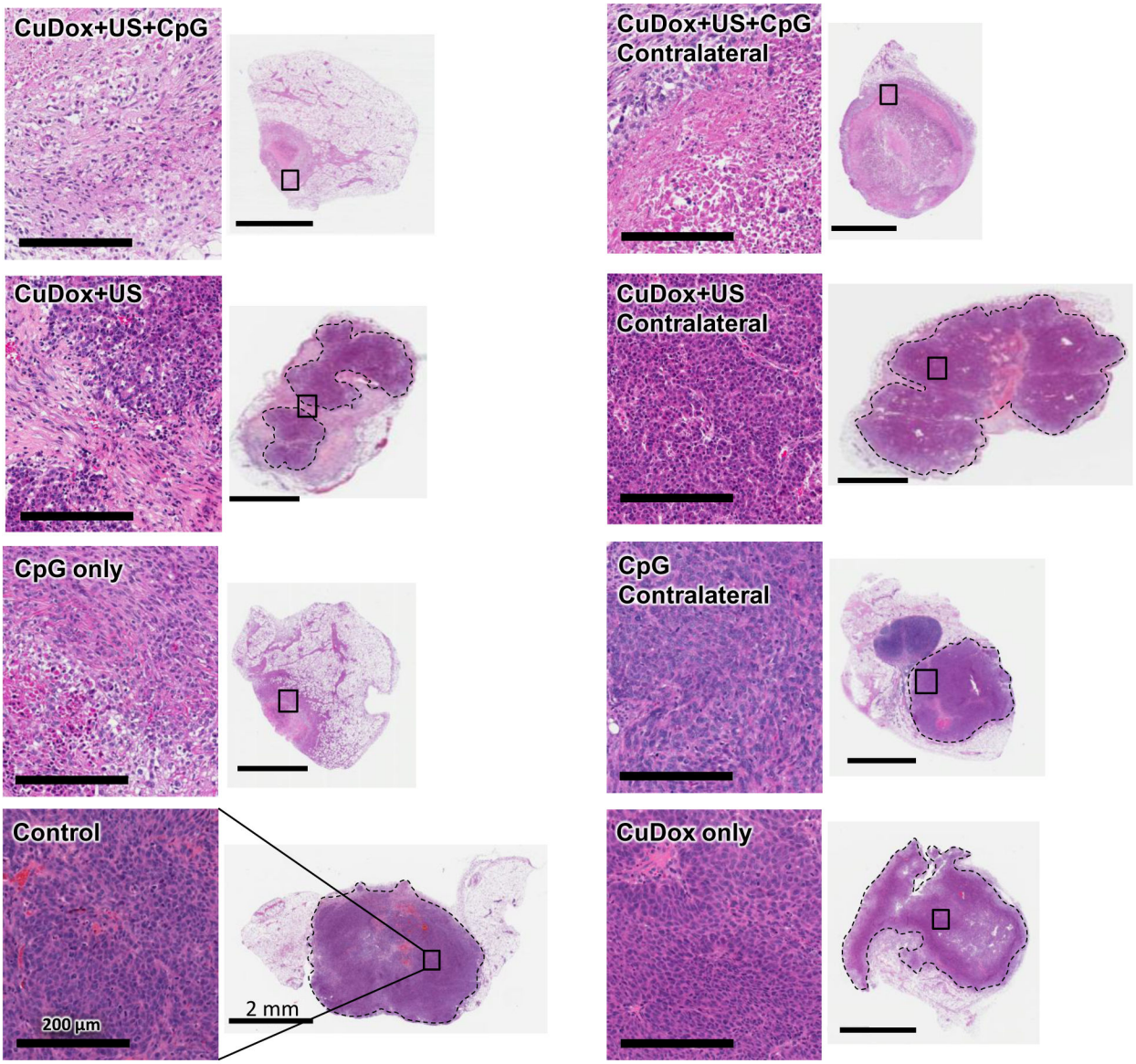

Fig. 2.

Histology of tumors treated with CuDox+US+CpG after the 10-day, 3-dose treatment period. H&E of representative NDL tumors from the #4 inguinal mammary fat pads of mice treated with CuDox+US+CpG, CuDox+US, CpG only or CuDox only compared to control tumors. Whole tumor sections (right panels in each column) and the magnified views enclosed by black boxes (left panels in each column) are shown. Areas enclosed by the dotted lines indicate viable tumor. Scale bars correspond to 200 μm (magnified panels) and 2 mm (whole tumor panels).

A

	% CD45+ Cells	CD45+ Cell # (x10^5)
Control	23.3 ± 4.7	23.2 ± 4.7
CpG	40.2 ± 24.7	26.3 ± 20.2
CpG Contralateral	39.8 ± 20.8	24.6 ± 16.3
US+CpG	34.6 ± 7.1*	18.8 ± 5.2
US+CpG Contralateral	35.3 ± 11.6	28.4 ± 14.7
CuDox+US	53.7 ± 14.3 *	52.0 ± 22.4
CuDox+US Contralateral	43.2 ± 24.6	28.6 ± 11.8
CuDox+US+CpG	44.6 ± 14.4 *	15.1 ± 8.3
CuDox+US+CpG Contralateral	50.0 ± 16.3 *	35.3 ± 19.5

* $P < 0.05$, compared to Control

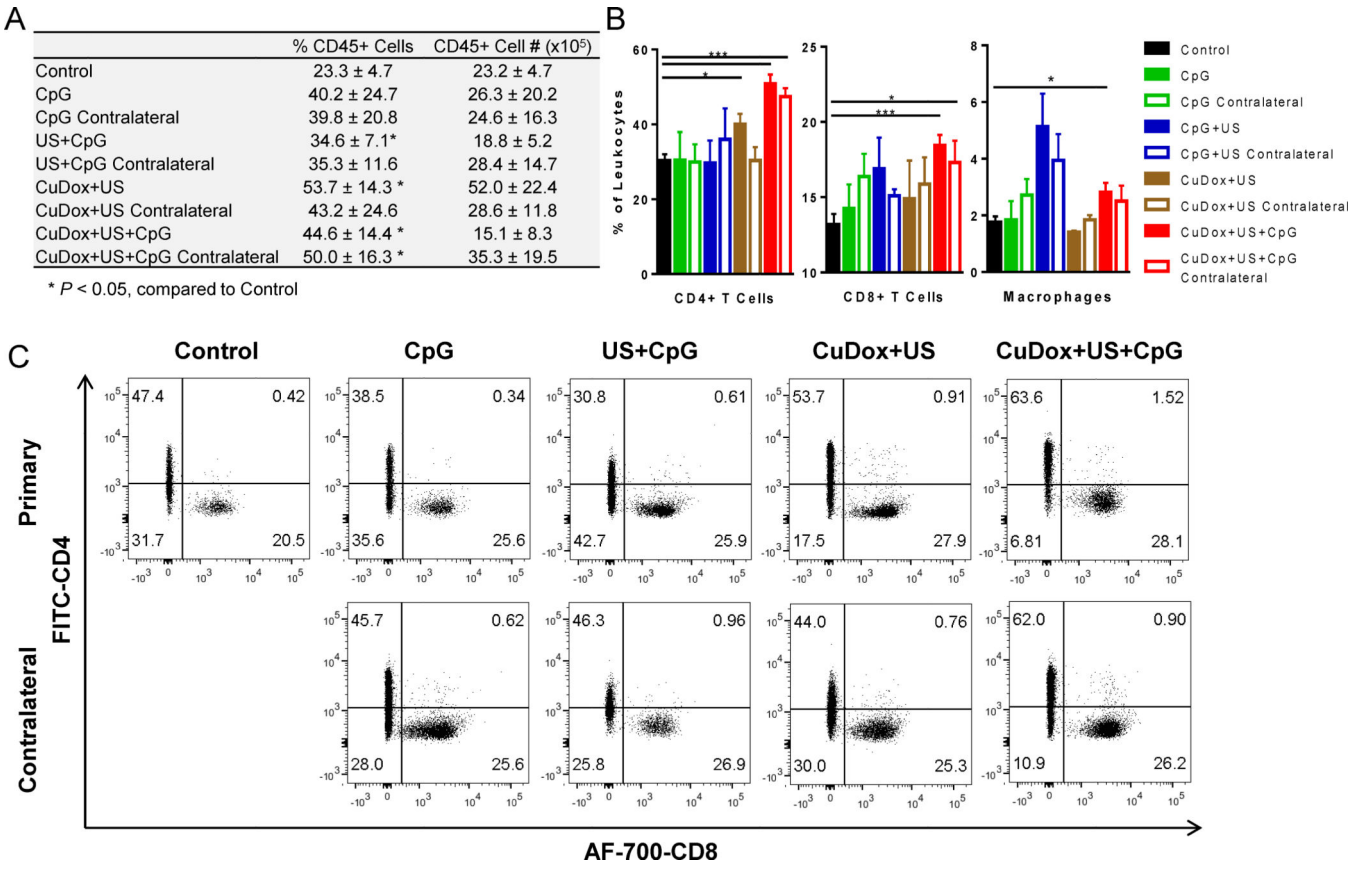

Fig. 3.

Tumor immune cell profiles at the termination of the 2-dose treatment period. Entire inguinal fat pads containing tumor and lymph node were harvested from treated mice and stained for CD45, CD3, CD4, CD8, F4/80, CD11b and Gr-1 on day 7 after the start of treatment and compared to untreated control mice via flow cytometry analysis. A: The percentage and total number of live cells positive for CD45 (leukocytes), given as mean ± SD. B: Frequencies of CD4+ T cells ($CD3^+CD4^+$), CD8+ T cells ($CD3^+CD8^+$) and macrophages ($CD11b^+F4/80^+Gr\text{-}1^-$), given as percentages of total leukocytes. Data shown are mean + SEM. C: Flow cytometry plots displaying frequencies of $CD45^+CD3^+$ pre-gated cells staining positive for CD4 or CD8 in each treatment group. Numbers in quadrants represent the percentages of cells positive for the indicated markers. After CuDox-TSL were injected in the tail vein, one tumor site per mouse was directly treated by US and/or CpG injection (“primary”); the contralateral site was not directly treated. The sample size was: control (n = 6), CpG (n = 4), US+CpG (n = 4), CuDox+US (n = 4), CuDox+US+CpG (n = 4). * $p < 0.05$, *** $p < 0.001$, two-tailed unpaired *t* test assuming unequal variance and Sidak-Bonferroni correction for multiple comparisons. Each treatment is compared only to the control.

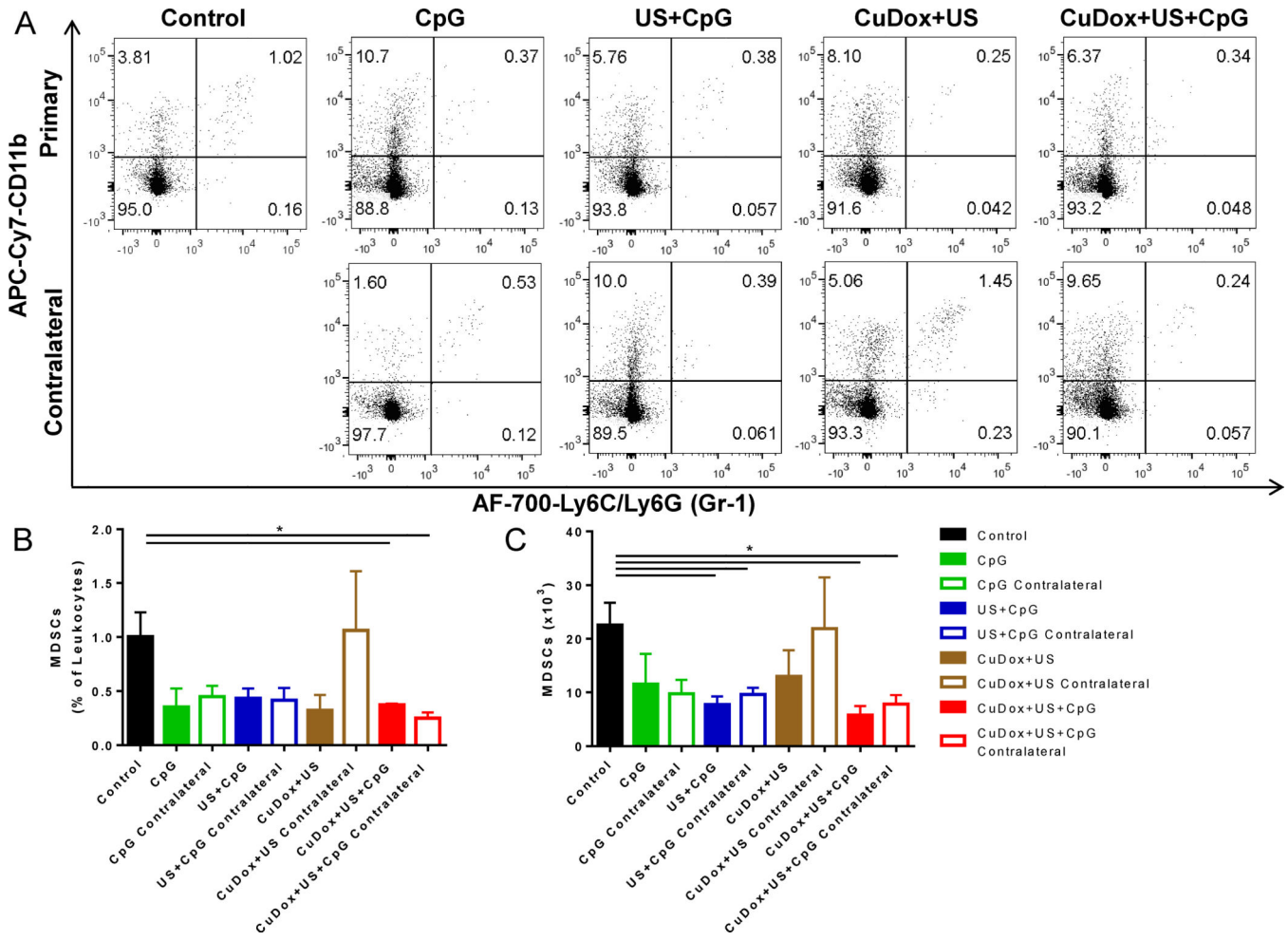

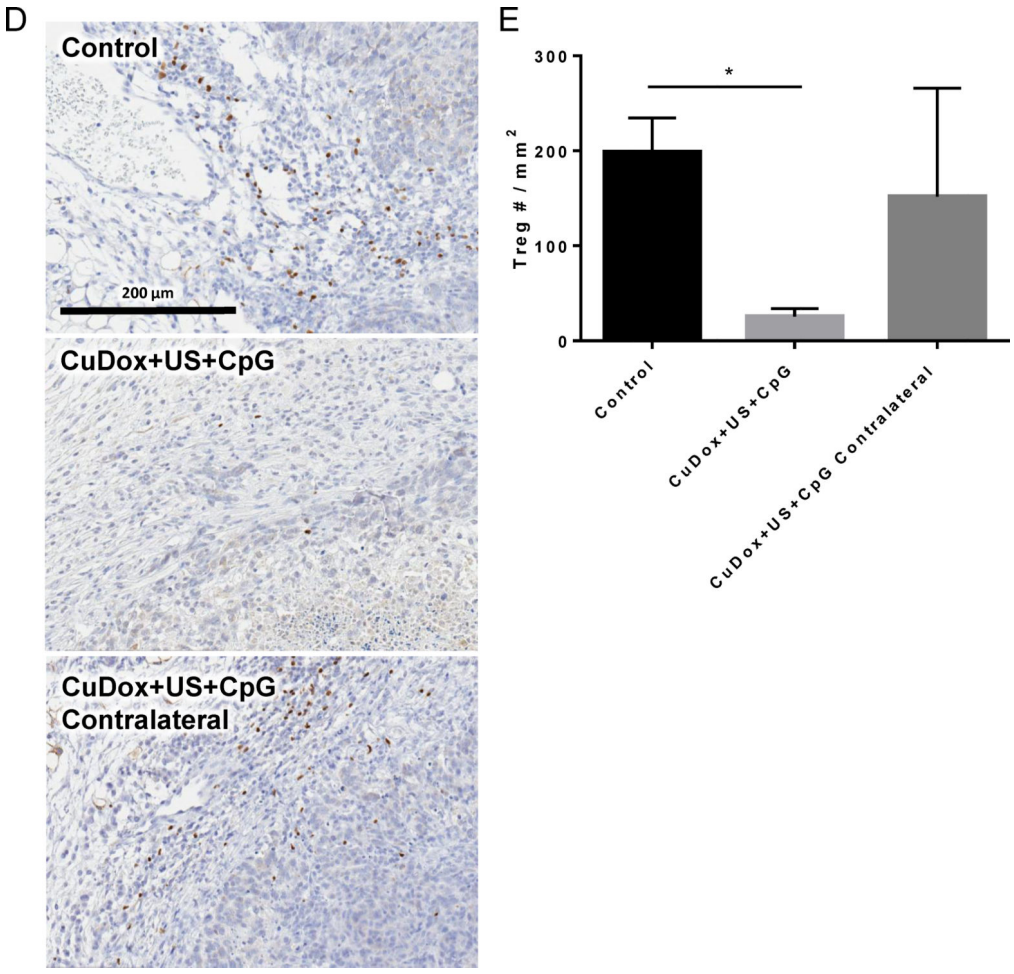

Fig. 4.

MDSCs and Tregs at the termination of treatment. A–C: Tumors/inguinal lymph nodes of treated mice were stained for CD45, CD11b and Ly6C/Ly6G (Gr-1) on day 7 after the start of treatment and analyzed via flow cytometry. A: Gated $CD45^+$ cells are shown in the flow cytometry dot plots and display frequencies of MDSCs positive for CD11b and Ly6C/Ly6G (Gr-1) in each treatment group. Numbers in quadrants represent the percentages of cells positive for the indicated markers. After CuDox-TSL were injected in the tail vein, one tumor site per mouse was directly treated by US and/or CpG injection ("primary"); the contralateral site was not directly treated. B: Frequencies of MDSCs ($CD11b^+Gr\text{-}1^+$) given as a percentage of total leukocytes and C: as total numbers. D: Treg staining in histological sections of fat pads containing tumor and inguinal lymph node on day 10 after 3 treatments. Sections were stained with Foxp3 (brown). E: Treg number/mm^2 in the periphery of tumors as quantified from histological sections. Data are shown as mean + SEM, * $p < 0.05$, two-tailed unpaired *t* test assuming unequal variance and Sidak-Bonferroni correction for multiple comparisons. Each treatment is compared only to the control. The sample size was: control (n = 6), CpG (n = 4), US+CpG (n = 4), CuDox+US (n = 4), CuDox+US+CpG (n = 4).

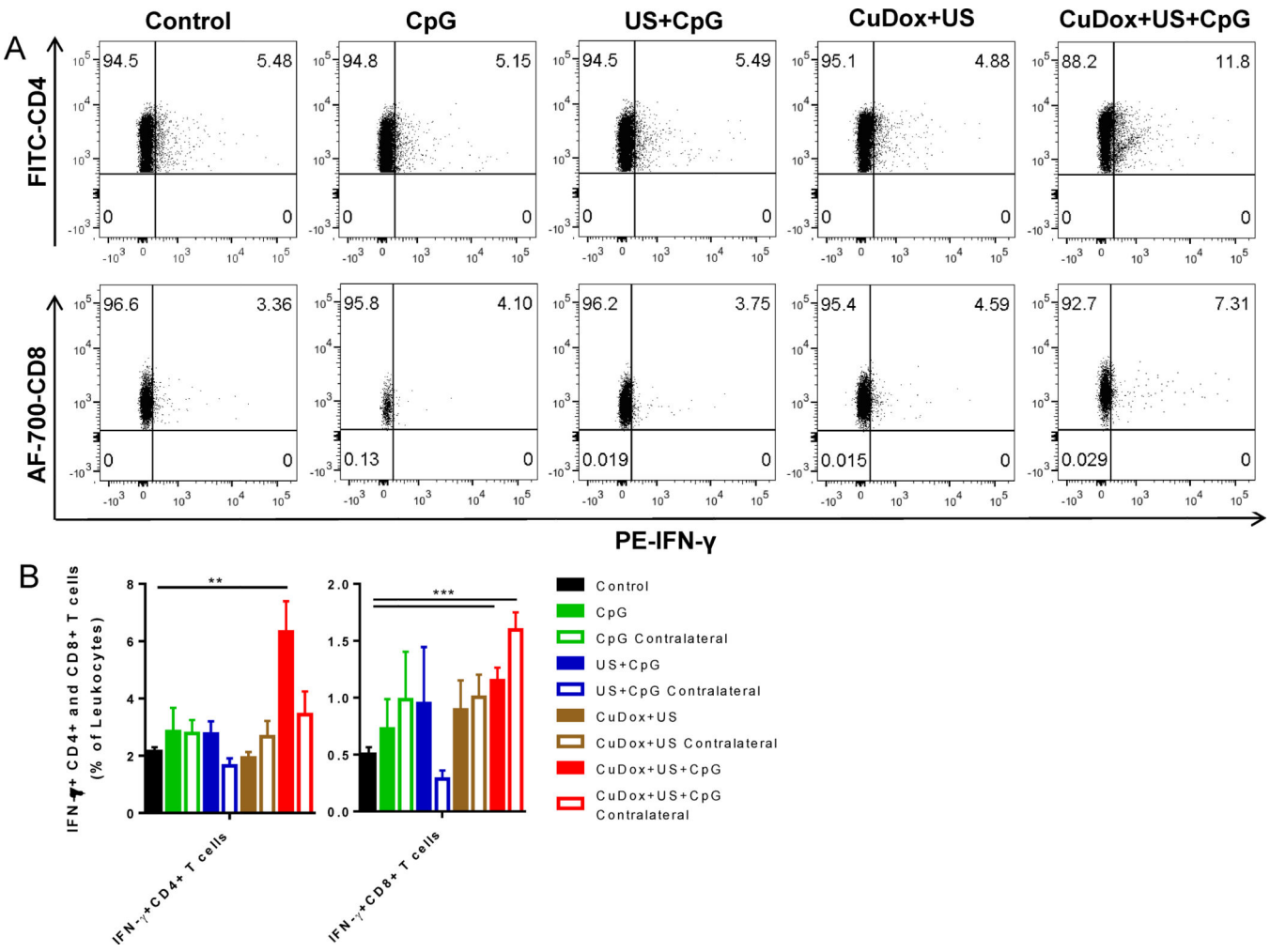

Fig. 5.

T-effector cell IFN-γ secretion in CuDox+US+CpG-treated tumor sites. Tumors/inguinal lymph nodes of treated mice were stained for CD45, CD3, CD4, CD8 and IFN-γ on day 7 after the start of treatment and compared to untreated control mice via flow cytometry. The sample size was: control (n = 6), CpG (n = 4), US+CpG (n = 4), CuDox+US (n = 4), CuDox +US+CpG (n = 4). A: Gated $CD45^+CD3^+$ cells are shown in the flow cytometry dot plots and display frequencies of cells double-positive for either CD4 and IFN-γ or CD8 and IFN-γ. Numbers in quadrants represent the percentages of cells positive for the mentioned markers. B: Frequencies of IFN-γ secreting CD4+ ($CD3^+CD4^+IFN\text{-}\gamma^+$) and CD8+ ($CD3^+CD8^+IFN\text{-}\gamma^+$) T cells given as a percentage of total leukocytes. Data are shown as mean + SEM, ** $p < 0.01$, *** $p < 0.001$, two-tailed unpaired t-test assuming unequal variance and Sidak-Bonferroni correction for multiple comparisons. Each treatment is compared only to the control.

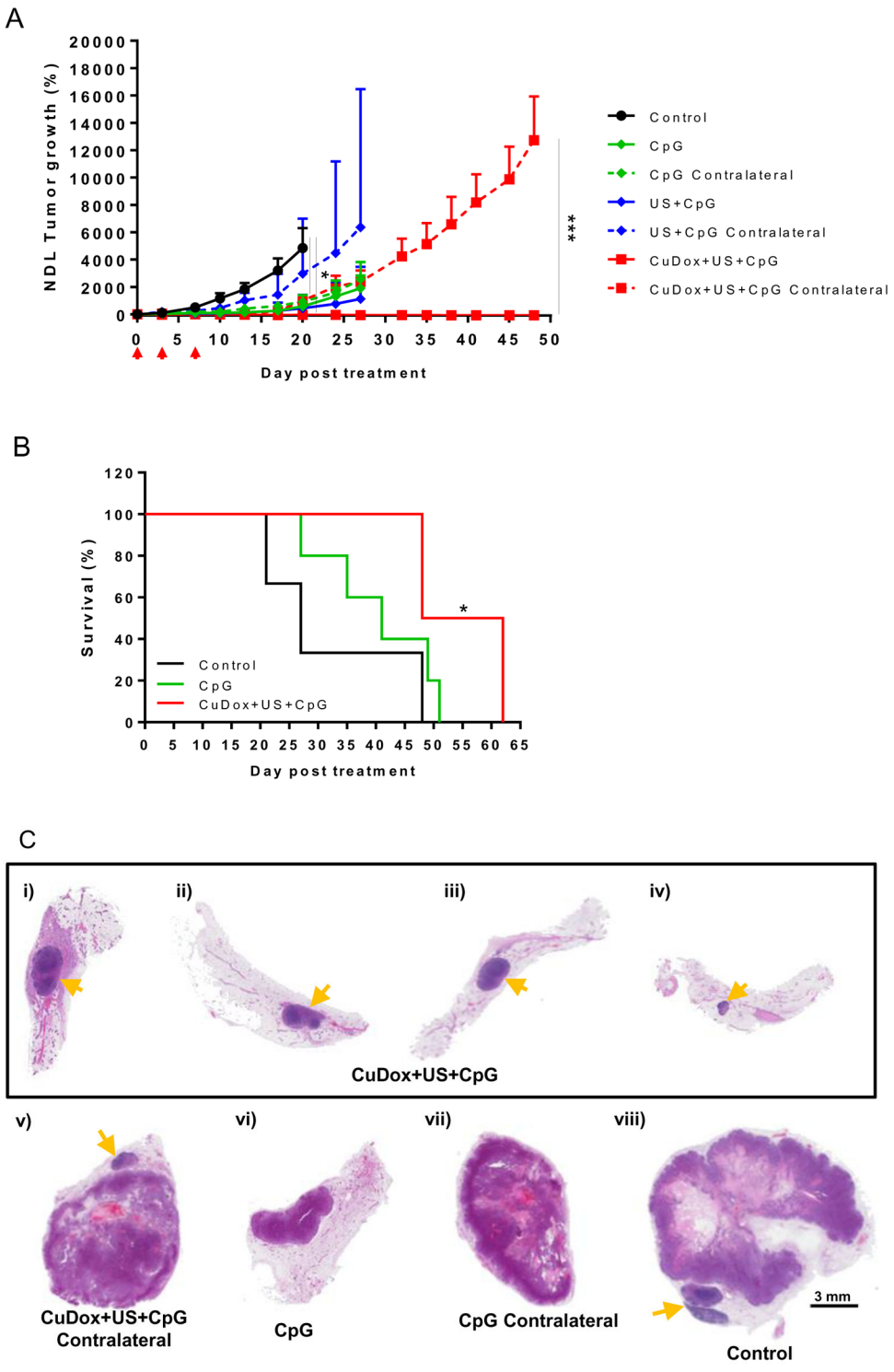

Fig. 6.

In vivo treatment efficiency of the immune adjuvant, CpG, with and without CuDox+US or US application. Mice received 3 treatments over the course of 10 days and were then monitored for up to 62 days. The sample size for this study was: control (n = 4), CpG (n =

7), US+CpG (n = 4), CuDox+US+CpG (n = 4). A: Tumor growth is quantified as a function of days after the start of treatment over the open-ended survival study period. Initial tumor diameter was ~4 mm. Directly-treated CuDox+US+CpG tumors maintain regression after treatment completion for the entire 48-day tumor-growth study duration. B: Kaplan-Meier survival plot. Survival of mice receiving CuDox+US+CpG was extended over the study period compared to control mice ($p = 0.024$). C: Tumor/fat pad histology at the termination of the open-ended survival study. H&E of whole NDL tumor sections from mice receiving CuDox+US+CpG (100 μg directly-treated tumors (i–iv), and representative contralateral tumor (v)) or 100 μg CpG (directly-treated tumor (vi) and contralateral tumor (vii)) compared to representative control tumor (viii). Viable tumor cells were not detected in the directly-treated CuDox+US+CpG tumors but were observed in all other treatment groups. Scale bar corresponds to 3 mm. Yellow arrows indicate lymph nodes. Data are shown as mean + SEM, * $p < 0.05$, One-way ANOVA with Tukey's post-hoc correction (A, day 20), *** $p < 0.001$, two-tailed unpaired *t* test (A, day 48). * $p < 0.05$, Log-rank statistics (B).